Characterization of *Fusarium circinatum* biofilm and its matrix's environmental response role

Francinah M Ratsoma
University of Pretoria https://orcid.org/0000-0002-0305-1327
Nthabiseng Z Mokoena
University of Pretoria https://orcid.org/0000-0002-5860-6959
Quentin C Santana
Agricultural Research Council https://orcid.org/0000-0002-1178-2533
Brenda D Wingfield
University of Pretoria https://orcid.org/0000-0002-6189-1519
Emma T Steenkamp
University of Pretoria https://orcid.org/0000-0003-0217-8219
Thabiso E Motaung (thabiso.motaung@up.ac.za)
University of Pretoria https://orcid.org/0000-0002-8813-7671

Research Article

Keywords: Biofilms, Fusarium circinatum, abiotic stress, antifungals, extracellular DNA, DNase

Posted Date: June 10th, 2023

DOI: https://doi.org/10.21203/rs.3.rs-3040583/v1

Abstract

The aggregation of fungal cells embedded in a matrix of extracellular matrix (ECM) results in a biofilm—a microbial community of sessile cells attached to biotic and/or abiotic surfaces. In this study, we demonstrate for the first time that the fatal pine pitch canker agent, *Fusarium circinatum*, can lead a biofilm-like lifestyle with aggregated hyphal bundles wrapped in ECM. We measured the biofilm ECM of *F. circinatum* in response to some key environmental factors. Our study suggests that *F. circinatum* biofilms respond to a changing environment, demonstrated by poor and optimal biofilm development under particular abiotic conditions, including temperature and pH. Further analysis revealed that while planktonic cells produced small amounts of ECM per unit of the biomass, azole-exposed biofilms produced significantly more ECM than non-exposed biofilms. The increased synthesis of ECM in biofilms due to azole exposure explains why *F. circinatum* biofilms required greater drug dosages (Imazalil: 0.74 mg/L; Tebuconazole: 0.46 mg/L) to kill 50% of biofilm-derived cells than planktonic cells (Imazalil: 0.26 mg/L; Tebuconazole: 0.04 mg/L). Interestingly, azole exposure based on these dosages also led to biofilms that were resistant to DNase, which typically uncouples biofilms by penetrating and degrading biofilm extracellular DNA; we propose that DNases were likely hindered from reaching target cells by the ECM barricade, a phenomenon prevalent in most biofilm-forming pathogens of humans. Therefore, our results show how an important fungal phytopathogen's sessile (biofilm) lifestyle could form a physical barrier against the surrounding environment.

Introduction

A biofilm is a microbial community of sessile cells attached to biotic and/or abiotic surfaces while embedding itself in a slimy heterogenous extracellular matrix (ECM) (Mitchell et al., 2016, Sheppard and Howell, 2016). ECM is mainly comprised of water and extracellular polymeric substances (EPS) such as carbohydrates, extracellular DNA (eDNA), lipids and proteins (Flemming and Wingender, 2010, Flemming et al., 2016). Because ECM is typically found between biofilm forming microbial cells, gluing them together (Beauvais et al., 2007, Flemming et al., 2016), it determines the three-dimensional architecture of biofilms. ECM also contributes to various additional properties differentiating biofilms from planktonic or free-living cells (Harding 2017, Motaung et al., 2020). These include enhanced tolerance to environmental challenges (e.g., in salinity and pH) and antimicrobial compounds (Karygianni et al., 2021; Harding 2017). Biofilm formation in filamentous fungi occurs through a succession of phases involving reversible and irreversible attachment, production of adhesive substances, microcolony formation, development and maturation to an ECM-enclosed structure from which fruiting bodies ultimately release spores for dispersal (Costerton et al., 1987; Costerton et a., 1999; McDougald et al., 2011).

The distinctive chemical and physical make-up of plant tissues present both a challenging and incentivising ecosystem for microbial colonists to form biofilms (Motaung et al., 2020). Indeed, ECM production, in association with plants and their biofilm forming colonists, has been reported by quite a number of studies (Harding et al., 2019). For example, phytopathogenic bacteria, such as *Pseudomonas syringae* pv. *phaseolicola* and *Curtobacterium flaccumfaciens* pv. *flaccumfaciens*, form biofilms on the

surfaces of dried bean seeds and sprouts that are accompanied by ECM production (Harding et al., 2019). In addition, several vascular pathogens (e.g., *Xylella fastidiosa* and *Ralstonia solanacearum*) clog their hosts' xylem vessels via ECM-embedded cells (Marques et al., 2002; Lowe-Power, 2018). *In planta* studies of fungal biofilms are rare, but it has been shown that *Aspergillus niger* infection in onion bulbs is associated with biofilms embedded within the ECM (Abdel-Aziz et al., 2019). Also, a range of plant-associated fungal pathogens produce biofilms under laboratory conditions (Harding et al., 2010; Peiqian et al., 2014), but very little is known about how biofilm formation, particularly ECM production, affects plant disease.

Here we investigated whether the filamentous fungus, *Fusarium circinatum*, is capable of biofilm production. *Fusarium circinatum* is notorious for causing resinous cankers on the trunks, branches and roots of trees, and root rot of seedlings in susceptible *Pinus* species (Martínez-Alvarez et al., 2014, Martín-Garcia et al., 2018; Wingfield et al., 2008). The fungus occurs in almost all regions where these plants are cultivated commercially, and in some areas, it also threatens natural *Pinus* stands (Zamora-Ballesteros et al., 2019; Drenkhan et al., 2020). The possibility that *F. circinatum* may live in a biofilm-like environment, which may form part of its virulence profile, has not been investigated. This is despite the fact that other economically important plant-associated members of the genus (e.g., *F. graminearum*, *F. verticillioides* and *F. oxysporum* f. sp. *cucumerinum*) form biofilms that are primarily distinguished by the production of ECM (Peiqian et al., 2014; Peremore et al., 2022; Shay et al., 2022).

Therefore, the study had two overarching aims. First, we explored the ability of *F. circinatum* to form surface-attached cultures, embedded within self-produced gelatinous matrixes similar to those exemplifying biofilms. Secondly, we examined how these structures, as well as their composition and activity, might be influenced by various abiotic factors. By making use of an array of laboratory and microscope-based approaches, we demonstrate that *F. circinatum* produce biofilms in vitro, and that their formation is significantly impacted by pH, carbon sources, temperature, and osmotic stress, suggesting that biofilm might be a type of adaptive strategy employed by *F. circinatum* under certain environmental conditions. We also show enhanced production of ECM in the presence azole fungicide and DNase, which implies that azole-induced ECM production provided protection against eDNA degradation. This is the first study to link ECM and eDNA to an antifungal response in phytopathogenic fungi, thus greatly improving the knowledge of *F. circinatum* biology and revealing a previously unrecognized antifungal resistance strategy.

Materials and Methods

Isolates and growth conditions

For this study, isolate FSP34 of *F. circinatum* was selected because it is highly pathogenic on *Pinus* (De Vos et al., 2011) and a wealth of biological information on this strain has been accumulated over the last two decades (e.g., Desjardins et al., 2000; Swalarsk-Parry et al., 2022; Phasha et al., 2021a, 2021b), making it an ideal model for the current study. This strain was obtained from the culture collection of the

Forestry and Agricultural Biotechnology Institute (FABI), University of Pretoria, South Africa. For routinely growing the fungus, it was cultured on potato dextrose agar (PDA) (Merck Group, Modderfontein GP, South Africa) for 7 days in the dark at 25°C. To obtain conidial cells, these cultures were flooded with 2 mL of phosphate-buffered saline (0.2 M PBS; 10 mM NaH_2PO_4, 10 mM Na_2HPO_4, 150 mM NaCl, pH 7.2). Conidia were counted in a Neubauer chamber and concentrations adjusted prior to use in downstream analyses.

Biofilm formation and visualization

To assess whether isolate FSP34 could form biofilms, 20 µL of conidial suspension (2 x 10^5 spores/mL) was added to 10 mL ¼ potato dextrose broth (PDB, Difco, Fisher Scientific, USA) in sterile 65mm petri dishes (ChemLab, SA) and incubated statically at room temperature (RT) for 7 days. Biofilm formation was also tracked over time according to Mowat et al. (2007), with slight modifications. Briefly, conidial suspensions in PDB (2 x 10^5 spores/mL) were incubated at room temperature (RT) for 24, 48, 72 h, and 7 days without shaking to allow conidia to settle and adhere to the bottom of the chamber slide (Nunc Lab-Tek II Chamber Slide System, Thermo Fisher Scientific). At the end of the incubation period, the broth was removed and the slide rinsed with distilled water to remove non-adhering cells. Metabolic activity of the biomass attached to the slides was then appraised using 2-chloro-4-(2,3-dihydro-3-methyl-(benzo-1,3-thiazol-2-yl)-methylidene)-1phenylquinolinium iodide (FUN-1; Invitrogen, Waltham, MA, USA), while ECM production was assessed with the cell wall polysaccharide-binding fluorescent dye concanavalin A-Alexa Fluor 488 conjugate (CAAF). This was achieved by flooding the rinsed slide with 200 µL of a solution containing 25 ug/mL of CAAF (Thermo-Fisher Scientific) and 25 ug/mL of FUN-1 (Invitrogen, Waltham, MA, USA). The fluorescent dyes were discarded and the slides were rinsed with PBS and assessed using ZEISS confocal laser scanning microscope 880 (CLSM), with excitation at 488/543 nm and emission at 505/560 nm for FUN1 and CAAF, respectively, using the 63x oil immersion lens (Laboratory for Microscopy and Microanalysis at University of Pretoria).

Biofilms were subjected to scanning electron microscopy (SEM) for structural analysis. For this purpose, sterile 65 mm mm petri dishes containing glass coverslips and 200 mL PDB were inoculated with 20 µL conidial cells (to a final concentration of 2 x 10^5 cells /mL) and statically incubated at RT for 7 days. Glass slides were then removed and flooded and rinsed with a PBS solution prior to adding the pre-fixative solution containing 1 mL of 2.5% (v/v) glutaraldehyde (Merck, South Africa) / formaldehyde (Merck, South Africa) and rinsed with PBS, after which the biofilms were fixed with 1% osmium tetroxide for 1 h. Following a final rinse with PBS, the fixed biofilms were dehydrated sequentially using a series of graded ethanol (i.e., 15 minutes rinses each in 1 mL ethanol at concentrations of 30%, 50%, 70%, 90%, and three rinses in absolute ethanol). The dehydrated samples were then treated with a 50:50 mixture of hexamethyldisilazane (HMDS) and absolute ethanol for 1 h, followed by a treatment with HMDS only, after which they were left to dry overnight. The glass slides were mounted on a rectangle aluminium stubs and carbon coated for 15 min using Qourum Q150T ES sputter coater (Qourumtech, UK). The stubs were observed in a JEOL JSM 6490LV scanning electron microscope (GenTech Scientific Inc., Arcade, NY, USA).

Biofilm biomass, metabolic activity, eDNA and ECM production

Crystal violet (CV) is commonly used to quantify the biomass of biofilms; this basic dye stains cells and their surrounding biofilm matrix (Ommen et al., 2017). Therefore, biofilm biomass of *F. circinatum* was quantified using CV staining as described previously (Peeters et al., 2008, Bhandari et al., 2021). For biofilm formation, a 96-well flat-bottom polystyrene plate (Thermo-Fisher Scientific) containing 200 µL of ¼ PDB was inoculated with FSP34 conidia to a final concentration of 2 x 10^5 cells/mL and incubated statically for 7 days at RT. For comparative purposes, another plate was prepared in the same way, but incubated with shaking at RT for 7 days to asses biomass production for planktonic cells. Biofilms were then rinsed with PBS to remove loose cells and plates containing planktonic cells were centrifuged (10 000 x *g* for 10 min at 4°C) and the supernatants discarded. In both cases, cells were fixed with 99% methanol for 15 min, after which the methanol was removed and plates air-dried (5 min). Fungal biomass in each well was then stained with 0.4% (w/v) crystal violet (Sigma-Aldrich, St Louis, MO, USA) dissolved in absolute ethanol. Following incubation at RT for 30 min, samples were rinsed twice with PBS to remove any unbound crystal violet. The biomass in each well was then decolorized by incubation at RT for 5 min in 200 µL absolute ethanol, after which absorbance was measured at 540 nm using a microplate reader (SpectraMax paradigm, Multimode detection platform).

Metabolic activity was assess using the tetrazolium XTT [2, 3-bis (2-methoxy-4-nitro-5-sulfophenyl)-2H-tetrazolium-5-carboxanilide] reduction assay (Roehm et al., 1991). It was performed on biofilm grown in 96-well flat-bottom polystyrene plates, as described above, while 5 mL of planktonic cells were shaken in 50 mL Erlenmeyer flask and 100 µL transferred to 96-well plate on the day of analysis. This was performed over a period of 72 h and 7 days. Following removal of excess broth and rinsing with PBS metabolic activity was evaluated using the Roche Cell Proliferation Kit II (Merck, South Africa). After incubation at 37°C in the dark for 3 h, colorimetric changes were measured at 492 nm using a microplate reader.

For ECM analysis, 7-day old biofilms and planktonic cultures were prepared in 96-well flat-bottom polystyrene plate as described above. ECM production was assayed in both cell types according to Choi et al. (2015) with slight modifications (Peng, 2016). Then, nonfixed biofilms were stained with 200 µL of 0.1% (w/v) basic fuchsin (Sigma-Aldrich), which binds to the polysaccharides of the biofilm, for 5 min at RT. The wells were then washed with PBS until the supernatants were translucent. The ECM was decolorised with 200 µL absolute ethanol and measured at 530 nm using a microplate reader (SpectraMax paradigm, Multimode detection platform).

eDNA contributes to the stabilization of the extracellular matrix (Rajendran et al., 2013). During this study, we wanted to determine whether the same is true for *F. circinatum* biofilms. Biofilms were grown as described above in sterile petri-dishes with PDB for 7 days at 25°C. After incubation, the biofilm was washed with 0.2 M PBS (pH 7.2). The disaggregated biofilm was then treated with 0.2 M EDTA (pH 8) to extract the ECM. The samples were then centrifuged at 10,000 x *g*, and the EDTA supernatant was

recovered and filtered using a 0.45-µm syringe filter (Millipore). eDNA was then extracted from the supernatant using Quick-DNA Fungal/Bacterial Kit (Zymo Research) following the manufacturer's instructions. The quantity of eDNA released onto the ECM was determined through a fluorescence assay using the DNA binding dye SYBR® Green I (Invitrogen), as previously described by Rajendran et al. (2014). Briefly, SYBR® Green I was added to the extracted DNA supernatants in a black well microtiter plate (Sigma-Aldrich) at a ratio of 1:1. The levels of eDNA were quantified using a fluorescence plate reader (SpectraMax paradigm, Multimode detection platform) at excitation 485 nm and emission 535 nm. The concentration of eDNA in the sample was extrapolated from the standard curve as previously described (Leggate et al., 2006). Then, early and late maturation biofilms formed at 72 h and 7 days, respectively, were subjected to DNase I (bovine pancreas) treatment (0.5 mg/ml) (Merck, South Africa).

Influence of pH, temperature, carbon source and osmotic stress

The impact of abiotic factors was quantified using the XTT reduction assay as described above. For these experiments, 96-well flat-bottom polystyrene plates containing 200 µL of ¼ PDB were inoculated with the conidia of isolate FSP34 to a final concentration of 2 x 10^5 cells /mL and incubated at RT over a period of 72 h and 7 days. Different pH values (2, 3, 4, 6, 7, 8) adjusted with HCl and 10 M NaOH.

To this end, a standardized spore suspension of the FSP34 isolate was inoculated in ¼ PDB and the effects of temperature (4, 15, 25, 30, 37°C) were evaluated over a period of 72 h and 7 days. Additionally, heat treatment (30 minutes to 1 hour) at 45°C was also applied to biofilms and planktonic cells produced as before. Both cell types were then let to grow for 72 h and 7 days and assessed as before using the cell proliferation kit II (Merck, South Africa).

The effect of sugars on biofilm formation was evaluated as described by Peiqian et al., (2014). Briefly, standardized spore suspension of the FSP34 isolate was inoculated in 96-well plate a minimal medium (20 mg/mL thiamine-HCL, 30 mM glucose, 26 mM glycine, 20 mM $MgSO_4$_$7H_2O$, and 58.8 mM KH_2PO_4) containing sugar sources including 30 mM glucose, maltose, lactose or sucrose over a period of 72 h and 7 days at RT. For osmotic stress, spores were inoculated in ¼ PDB containing 1 M NaCl or 1.5 M sorbitol 72 h and 7 days at RT.

Biofilm response to azole fungicides

We first determined the concentrations at which two commercially available fungicides, Imazalil and Tebuconazole, inhibited the radial growth on PDA by 50% (I_{50}) The fungicides were suspended in sterile distilled water and added to PDA post sterilization (50°C) at the concentrations 0, 0.1,1,10 and 100 mg/L. Mycelial plugs (5mm), taken from the margins of 7-day old PDA cultures with the aid of a cork borer, were then placed at the centre of the 90 mm Petri plates (with the mycelium facing towards the medium). Six biological replicates were prepared per concentration of the fungicide to which isolates were exposed. The plates were incubated in the dark for 7 days at 25°C. Following growth, the colony diameter was measured using a metric ruler with the plates marked with perpendicular axes. Percentage of inhibition at

the different fungicide concentrations was then calculated as (B1–B2)/B1 x 100, where B1 is the radial growth of the fungus in the absence of fungicide and B2 the radial growth in the presence of fungicide.

The response of biofilms to Imazalil and Tebuconazole was performed according to Ramage et al., (2011) using 96-well plates. Briefly, individual wells containing 200 µL of PDB and fungicide (0, 0.1,1,10 and 100 mg/L) were inoculated with FSP34 conidial cells to a final concentration of 2 x 10^5 cells /mL. Following static incubation for 7 days at RT, the inhibition percentage was determined using crystal violet assay performed on the biofilms as described previously. Wells with only broth were treated as negative controls, broth and conidia without treatment were treated as positive control (PC), while broth with fungicides were used as contamination control. Percentage inhibition was determined as $(C_1 – C_2)/C_1$ x 100, where C_1 is the growth of biofilm absence of fungicide and C_2 the biofilm growth in the presence of fungicide.

Concentrations inhibiting 50% (I_{50}) growth were used to assess metabolic activities of planktonic and biofilm cells using the cell proliferation kit II (Merck, South Africa), as well as the biomass and ECM production as described above at time points 72 h and 7 days on newly formed biofilms which were treated with fungicides overnight prior to analysis. In addition, the digestion of eDNA was also performed order to determine whether DNase I predisposes the biofilm to antifungal attack. In this experiment, the pre-formed biofilms (72 h or 7 days, independently) were treated with DNase I and incubated for 24 h at RT prior to analysis. Heat inactivated (75°C for 15 min) DNase I (DNase-) and biofilms treated with or without azoles (Imazalil and Tebuconazole) were used as negative controls.

Reproducibility and statistical analyses

Data is presented as mean ± standard error of the mean (SE). Statistical analyses were performed using GraphPad statistical software (GraphPad 5 Software, San Diego, CA, USA). Images were captured using the Epson scanner (Epson perfection V700 photo). For statistical analysis of viable counts, cultures containing 2 x 10^5 CFU/ ml were used. All obtained data in the assays unless stated were compared using one way ANOVA and non-parametric student t-test analysis. Statistical significance levels were defined as $p > 0.05$ = not significant (ns) or either $p < 0.01$ (a, b, c or x, y, z) respectively. All experiments we performed in triplicates except for the mycelial antifungal studies which included six biological replicates.

Results

In this study, *F. circinatum* formed cloudy biofilm like structures in petri dishes containing ¼ strength PDB (Fig. S1, A). CLSM was used to investigate further the ability of the isolate to form biofilms through the different phases using the red FUN1 dye which stain metabolically active cells red while the green fluorescence CAAF depict secretion of ECM (Fig. 1). The initial phase of biofilm formation was at 24 h, and exhibited an aggregate of actively germinating conidia, shown by red florescence (FUN1 stain; Fig. 1A). During early maturation at 48 h, the biofilm was characterized by microcolony formation with pronounced hyphal growth and demonstrated a more yellowish fluorescence (combination of both FUN1

and CAAF stains) (Fig. 1B), possibly in preparation for secretion of the ECM. However, regions lacking green fluorescence (CAAF stain) were observed, which meant that no ECM could be detected. The maturation of the biofilm (72 h, Fig. 1C) showed compacted hyphal networks stuck together by secreted ECM (green fluorescence- CAAF stain). The dispersal phase (7 days, Fig. 1D) exhibited hyphal bundles embedded in the ECM (largely stained by the CAAF stain) with some released conidial cells (arrow), typical of the dispersal stage.

According to SEM imaging analysis, *F. circinatum* FSP34 isolate forms dense and tightly packed mass of mycelial mat with innumerable interconnected hyphae (Fig. 2A). SEM images further revealed the presence of inner channels interwoven like a trap, but did not reveal any ECM, which is a hallmark of biofilm formation. We hypothesized that the reason for not observing ECM is that biofilms typically develop in response to stress conditions, which explains their recalcitrance to extreme environments (Motaung et al., 2020). Correspondingly, we observed that the ECM was not detectable under microscopic examination when the biofilm was incubated without any stress condition (Fig. 2A). Due to this lack of observable ECM, the biofilm could not be distinguished from planktonic cells (Fig. 2B), suggesting that a fully-fledged biofilm is formed in the presence of stress. To investigate our hypothesis, we subjected *F. circinatum* spores at stationary phase to heat-shock treatment at 45°C, upon which the ECM became more visible, resembling a glue-like substance (Fig. 2C). This observation aligns with previous reports on the physical appearance of ECM in biofilms (Peremore et al., 2022), strongly suggesting that the FSP34 biofilm undergoes a response mediated by the ECM. To further confirm the formation of biofilms in *F. circinatum*, we evaluated three different parameters: crystal violet (CV) staining for cell wall components, basic fuchsin staining for nuclei and cytoplasmic granules, and XTT analysis for cell viability and metabolic activity. The results consistently demonstrated that under heat-shock, the biofilm exhibited a substantial production of ECM per unit of biomass relative to the control groups (Fig. 2D). These findings provide additional evidence supporting the notion that *F. circinatum* releases ECM in response to a stress condition. The metabolic activity of planktonic cells was also significantly reduced compared to that of biofilms (Fig. 2E; $P < 0.0001$). Taken together, our findings clearly indicate fundamental differences in the general biology of the two cell types and strongly suggest that *F. circinatum* is capable of forming true biofilms when confronted with stress.

Fusarium circinatum biofilms respond to various abiotic factors

The effect of pH, temperature, sugars, and osmotic stresses on the ability of the FSP34 isolate to form a biofilm was quantified using the XTT reduction assay at two time points (72 h and 7 days), as illustrated in Fig. 3. In the aforementioned assay, high optical density (OD) is proportional to the amount of metabolically active cells, which corresponds to firmly or weaker attached biofilms. Overall optimal biofilm growth was observed at pH 6 at both time periods (Fig. 3A). Feeble biofilms were displayed at low metabolic activities under acidic pH (2, 3, and 4) conditions. Under alkaline conditions (pH 8), conidia used as inoculum failed to germinate into biofilms. At 4, 15, and 37°C (Fig. 3D), low to no metabolic activity was determined which indicated that no biofilms formed after 72 h. Biofilms formed at 25 and 30°C. Increased metabolic activity and biofilm formation was observed on day 7 at 15, 25, and 30°C,

while lower metabolic activity and biofilm formation was maintained at 4 and 37°C. High metabolic activity was observed on day 7 in the presence of glucose, lactose, and maltose indicating strong biofilm formation (Fig. 3B). Under osmotic stress conditions, biofilms developed in the presence of NaCl and sorbitol (Fig. 3C); with increased metabolic activity observed after 72 h in NaCl compared to sorbitol. Metabolic activity decreased significantly at day 7 under NaCl stress. A fluctuation of ECM production was observed under subjected conditions, at which most exhibited insignificant statistical differences compared to the positive control (Fig. S2 A-D).

Azoles increase matrix levels in *Fusarium circinatum* biofilms

During the analysis of azole effects on mature biofilms, we first compared the general response of planktonic and biofilms to Imazalil and Tebuconazole. The results suggested that both *F. circinatum* biofilms and planktonic cells were generally highly inhibited by both drugs, with Tebuconazole showing more inhibition than Imazalil (Fig. S3A). The biofilm, however, exhibited higher resistance to treatment when they were compared to planktonic cells and the untreated controls across all concentrations of Imazalil and Tebuconazole. To get a clear implication of this observation, we evaluated metabolic activity and ECM production per unit of biofilm biomass. The metabolic activity of the biofilms as well as the ECM produced was determined using identified Ic_{50} values (Table S1), in the presence of Imazalil (750 µg/L) and Tebuconazole (460 µg/L). The biofilm cells displayed high metabolic activity under azole treatment alone when compared to the untreated controls, particularly at 7 days (Fig. 4A). Additionally, the biofilm metabolic response was accompanied by a significant increase in ECM, which was not seen in the untreated control samples (Fig. 4B), in the presence of both azoles and at both 72 hours and 7 days. Biofilms appear to release substantial amounts of ECM in response to antifungals. This explains why the Ic_{50} values for both azoles are greater than those for planktonic cells and suggests that the tested azoles are less effective antifungal agents on biofilms (Table S1).

Azoles may interfere with DNase activity by increasing biofilm ECM levels

Exogenous application of DNase is known to reduce early biofilm development and tolerance to antimicrobials by deteriorating eDNA, an essential biofilm structural component (Whitchurch et al., 2002, Tetz et al., 2009). We reasoned that since both Imazalil and Tebuconazole boost ECM production during antifungal exposure (Fig. 4B), thus preventing these azoles from reaching target cells, the increasing ECM of mature biofilms could interfere with DNase activity by preventing penetration of the biofilm by the DNase. To investigate this possibility, we first verified that the use of DNase did, in fact, reduce the production of biofilms, as is usually the case in bacterial biofilms (Whitchurch et al., 2002, Tetz et al., 2009). Although there are few outliers, DNase is expected to have high antibiofilm efficiency during early biofilm formation because immature biofilms have a less complex architecture, with very little ECM (Tetz et al., 2009, Schlafer et al., 2018).

However, our analysis was limited to early and late biofilm development at 72 h and 7 days, respectively, because the *F. circinatum* biofilm is highly unstable at 24 h. Our research revealed that metabolic activity

was high in all the treatments (i.e., DNase plus azoles) during the 72 hours of maturation, probably mostly directed toward the formation of ECM as seen by the high levels of this complex (Fig. 5B). As the ECM serves as a shield, this may be done to counteract the effects of DNase and azole stress. Interestingly, metabolic activity remained higher in the $DNase^+$ sample despite being dramatically decreased throughout late development (7 days) (Fig. 5A). As a result, ECM synthesis in the $DNase^+$ sample increased just after 72 hours and sharply decreased 4 days later, meaning DNase can easily disperse a young *F. circinatum* biofilm (24–72 h) than an old and more complex biofilm (7 days). ECM levels, however, remained noticeably higher in the azole treatments, with a slight decrease in Tebuconazole (Fig. 5B). These results imply that azoles are the strongest inducer of ECM production during all growth phases and will likely contribute to the decreased efficacy of DNase.

Discussion

The presented data suggests, for the first time through *in vitro* processes that *F. circinatum* (FSP34) forms biofilms which may be associated with mechanisms of pathogenesis and survival under different abiotic stresses. *F. circinatum* biofilm formation follows the preliminary model of Harding et al., (2009) by filamentous fungi. By using the fluorescent dyes (FUN1 and CAAF), we observed that the morphological structures formed in liquid cultures demonstrated microcolony development; tightly packed hyphae; production of ECM and dispersal of planktonic cells (Fig. 1). Additionally, tightly packed homogenous mycelia with interwoven hyphae were observed (Fig. 2A), with the production of ECM covering hyphae only microscopically seen when the cells were exposed to heat treatment (Fig. 2C-D). Given the performance of biofilms under this condition, our findings suggest that *F. circinatum* biofilms are superior to their planktonic counterparts (Fig. 2E). Other studies have also described biofilm formation using similar techniques in fungi and bacteria (Chandra et al., 2001, Seidler et al., 2008, Harding et al., 2009). In addition, using the fluorescence dye SYBR Green 1, we determined that the ECM contained 0.64 ± 0.05 ng/µL of eDNA. The increased composition of biofilms may be owed to the fact that these structures play critical roles in protecting cells and maintaining the structural stability of the biofilm. Therefore, to a greater extend, these analyses support the notion that *F. circinatum* forms 'true' biofilms, which may be employed as a strategy to respond to a dynamic environment and stress.

Biofilms formation is affected by various environmental cues (i.e., pH, carbon sources availability, osmotic stress, and temperature). The formation *F. circinatum* biofilms was higher under neutral conditions as opposed to very acidic and alkaline pH conditions (Fig. 3A). Alarmingly, this suggests that *F. circinatum* can easily grow and form biofilms that colonize various susceptible tree species such as *P. patula*, which grows in temperate zones of pH ranging from 3.3 to 6.4 (Geffert et al., 2019). Notably, we also observed that biofilm formation of *F. circinatum* is dependent on the assimilation of nutrients such as glucose or lactose. Although glucose has been reported to be an efficient carbon source for nutrition and growth in microbes *in vitro* (Chew et al., 2019), we observed in this study that lactose showed optimal biofilm formation for *F. circinatum* (Fig. 3B). In other studies, the presence of lactose displayed variation of fungal growth (i.e., *Pestalotiopsis submerses* and *Tetracheatum elegans*) (Sati and Bisht, (2006).

Nonetheless, lactose is an important carbon source of cellulolytic enzyme, which is used as a biological weapon by a number of plant pathogens including *Fusarium* spp. to break down plant cell wall into simple sugars, which in this case may be used to further fuel the biofilm (Seiboth et., 2007; Chew et al., 2019).

Furthermore, microbes exposed to hostile environments (e.g., H_2O_2 and NaCl) undergo biofilm formation and produce EPS to protect cells in *Candida albicans*, the same has been reported in other bacterial species which formed biofilms in the presence of a stress condition (Zhang et al., 2007, Villa et al., 2012, Moryl et al., 2014, Pemmaraju et al., 2016). These findings are in line with our findings whereby *F. circinatum* formed biofilms in the presence of sorbitol and NaCl (Fig. 3C), although with marginal significance. Temperature is important for the initiation of biofilm formation, and we observed no biofilm attachment at temperatures 4,15, and 37°C in the first 72 h (Fig. 3D). Reminiscent with our findings, others have shown that *F. circinatum* does not grow at temperatures of 5 and 40°C but slight growth can be observed at 37°C (Mullett et al., 2017, Elvira-Recuenco et al., 2021). Interestingly, the *F. circinatum* biofilm seems to attach and form at the optimal temperature of 15°C. We speculate that the increased formation of the biofilm at such low temperatures may be used by the fungus as a shield from the cold.

In this study, we used common agricultural azole fungicides (i.e., triazoles and imidazoles). These agents target ergosterol biosynthesis by inhibiting the activity of a cytochrome P450 enzyme, ergosterol 14-α-demethylase (CYP51/ERG11) and have been reported for their efficacy against *Fusarium* spp. (Audenaert et al., 2011, Odds et al., 2011, Tini et al., 2020). Studies have shown that planktonic cells are generally more susceptible to fungicides than biofilms (Peiqian et al., 2014, Berbegal et al., 2015). Resistance of fungal biofilms against antimicrobial treatments involves the matrix, efflux pump, and persisters (Sardi et al., 2014, Kaur and Nobile, 2023). There is very limited knowledge regarding the mechanisms of antifungal resistance in *F. circinatum*. We observed that *F. circinatum* biofilms showed resistance towards Imazilil and Tebuconazole (Fig. S3A) and, in response to these azoles, produced more ECM (Fig. 4B). A similar trend was observed in *C. albicans* biofilms with high expressions of the *FKS1* gene exposed to antifungal drugs resulted in increased levels of biofilm matrix secretion (Nett et al., 2010). In both cases, acting as a barricade, increased ECM production prevents the diffusion of the antifungal drugs, suggesting that the ECM may play a role in antifungal resistance across fungal species. Therefore, ECM production may be a potential biomarker for antifungal resistance, if identified in field isolates. The presence of azoles greatly lower metabolic activity in cells when present in media (Fig. 4A; 7 days); these biofilms are likely made up of dormant, dying, or dead cells since they are rather old. Living cells can consume dead cells as a source of nutrients (López et al., 2011), which can promote the formation of ECM and further improve biofilm development.

To understand the contribution of eDNA in *F. circinatum* biofilms with regards to antifungal sensitivity, DNase was used to treat pre-formed biofilms. We reveal that *F. circinatum* biofilms, in terms of metabolic activity, were not inhibited by DNase (Fig. 5A). However, DNase seemed to have a great impact on the production of ECM and biomass. Indeed, we observed resistance and high production of ECM in the presence of DNase plus antifungals (Fig. 5B). This implies that additional eDNA excreted, possibly from

dead or dying cells, likely competes with the DNase that we supplied in the media, allowing the biofilm to produce high amounts of ECM and survive despite the simultaneous stress of DNase and azoles. Seemingly, soil environments also contain mass amounts of active extracellular DNases, which are involved in the recycling of eDNA (Foucher et al., 2020, Yang et al., 2022). In addition, fungi and bacteria in the environment may produce extracellular DNases to carry out specific crucial functions that are advantageous to the microorganism. For instance, DNase in the maize fungal pathogen, *Cochliobolus heterostrophus*, contributes to virulence presumably by degrading plant eDNA, which is crucial for plant immunity (Monticolo et al., 2020) The Type six secretion system of Gram-negative bacteria can also send an effector called TafE (ACX6015365), which is a Mg^{2+}-dependent DNase that kills fungi by degrading their DNA (Luo et al., 2022). This system is highly active and influences how predator and prey cells compete within the biofilm (Teschle et al., 2022). Together, these findings support the hypothesis that extracellular DNases are present in the environment and that microbial biofilms may be continuously exposed to them, warranting microbes such as fungi to establish mechanisms that combat this "DNase stress". We argue that one of these mechanisms may involve increasing the amount of ECM to stop DNase from penetrating the biofilm, reaching target cells, as highlighted in this study (Fig. 5B). Therefore, the application of fungicides may potentially enact an opposite effect of what it was intended to when it comes to biofilms, the biology of which the majority of plant pathologists have no clue; these fungicides, based on presented data, seem to encourage the production of ECM and biomass, further preventing natural pathogen control through DNases coming from the environment. In this case, natural pathogen control means that environmental DNases cannot work to control pathogens, as artificial/chemical interventions using fungicides oppose this natural effort. Therefore, DNase cannot be used as a potential antibiofilm therapy to remove plant-associated biofilms, especially in the presence of azole fungicides.

In conclusion, our study showed that the *F. circinatum* forms ‘true’ biofilms. We found that the formation of biofilms is affected by external factors. *F. circinatum* biofilms are not only resistant to high heat but also tested azole agents. The use of DNase with azole against the biofilm showed increased ECM production and resistance to azoles. *F. circinatum* remains economically important worldwide, therefore these results will be useful in improving management strategies especially in designing fungicides that target biofilm cells to combat both the planktonic and biofilm phases of the fungus.

Declarations

Credit authorship contribution statement

Francinah M Ratsoma: Conceptualization, methodology, investigation, analysis, writing-original draft, writing manuscript and editing. Nthabiseng Z Mokoena: Investigation and analysis Quentin Santana: Editing. Brenda Wingfield: Conceptualization, methodology, and editing. Emma Steenkamp: Conceptualization, methodology, investigation, analysis, and editing. Thabiso E Motaung: Conceptualization, methodology, editing manuscript and editing, resources, supervision, and funding acquisition.

Funding details.

National Research Foundation (South Africa) under the Thuthuka funding instrument (Grant no. 129580) and the DSI-NRF *Centre* of Excellence in *Plant Health Biotechnology* (CPHB, previously the *CTHB*).

Conflict of interest.

None

References

Abdel-Aziz, M.M., Emam, T.M. and Elsherbiny, E.A., 2019. Effects of mandarin (Citrus reticulata) peel essential oil as a natural antibiofilm agent against *Aspergillus niger* in onion bulbs. *Postharvest Biology and Technology*, 156, p.110959.

Anon. 2018. Forestry and Forest Products Industry Facts – 1980 to 2018. Available at http://www.forestrysouthafrica.co.za/wp-content/uploads/2019/12/Forestry-FP-Industry-Facts-1980-2018.pdf [accessed 12 September, 2022]

Audenaert, K., Landschoot, S., Vanheule, A., Waegeman, W., De Baets, B. and Haesaert, G., 2011. Impact of fungicide timing on the composition of the Fusarium head blight disease complex and the presence of deoxynivalenol (DON) in wheat. *Fungicides-Beneficial and Harmful Aspects*, pp.79-98.

Beauvais, A., Schmidt, C., Guadagnini, S., Roux, P., Perret, E., Henry, C., Paris, S., Mallet, A., Prévost, M.C. and Latgé, J.P., 2007. An extracellular matrix glues together the aerial-grown hyphae of *Aspergillus fumigatus*. *Cellular microbiology*, *9*(6), pp.1588-1600.

Berbegal, M., Landeras, E., Sánchez, D., Abad-Campos, P., Pérez-Sierra, A. and Armengol, J., 2015. Evaluation of *Pinus radiata* seed treatments to control *Fusarium circinatum*: effects on seed emergence and disease incidence. *Forest Pathology*, 45(6), pp.525-533.

Bezos, D., Martinez-Alvarez, P., Fernandez, M. and Diez, J.J., 2017. Epidemiology and management of pine pitch canker disease in Europe—A review. *Balt. For*, 23, pp.279-293.

Bhandari, S., Khadayat, K., Poudel, S., Shrestha, S., Shrestha, R., Devkota, P., Khanal, S. and Marasini, B.P., 2021. Phytochemical analysis of medicinal plants of Nepal and their antibacterial and antibiofilm activities against uropathogenic *Escherichia coli*. *BMC Complementary Medicine and Therapies*, *21*, pp.1-11.

Casagrande Pierantoni, D., Corte, L., Casadevall, A., Robert, V., Cardinali, G. and Tascini, C., 2021. How does temperature trigger biofilm adhesion and growth in *Candida albicans* and two non-*Candida albicans* Candida species?. *Mycoses*, 64(11), pp.1412-1421.

Chew, S.Y., Chee, W.J.Y. and Than, L.T.L., 2019. The glyoxylate cycle and alternative carbon metabolism as metabolic adaptation strategies of Candida glabrata: perspectives from *Candida albicans* and *Saccharomyces cerevisiae*. *Journal of biomedical science*, 26, pp.1-10.

Choi, N.Y., Kang, S.Y. and Kim, K.J., 2015. *Artemisia princeps* inhibits biofilm formation and virulence-factor expression of antibiotic-resistant bacteria. *BioMed research international*, 2015.

Córdova-Alcántara, I.M., Venegas-Cortés, D.L., Martínez-Rivera, M.Á., Pérez, N.O. and Rodriguez-Tovar, A.V., 2019. Biofilm characterization of *Fusarium solani* keratitis isolate: increased resistance to antifungals and UV light. *Journal of Microbiology*, 57(6), pp.485-497.

Corte, L., Casagrande Pierantoni, D., Tascini, C., Roscini, L. and Cardinali, G., 2019. Biofilm specific activity: a measure to quantify microbial biofilm. *Microorganisms*, 7(3), p.73.

Costa, O.Y., Raaijmakers, J.M. and Kuramae, E.E., 2018. Microbial extracellular polymeric substances: ecological function and impact on soil aggregation. *Frontiers in microbiology*, 9, p.1636.

Costerton, J.W., Cheng, K.J., Geesey, G.G., Ladd, T.I., Nickel, J.C., Dasgupta, M. and Marrie, T.J., 1987. Bacterial biofilms in nature and disease. *Annual Reviews in Microbiology*, *41*(1), pp.435-464.

Costerton, J.W., 1999. Introduction to biofilm. International journal of antimicrobial agents, 11(3-4), pp.217-239.Desjardins, A.E., Plattner, R.D. and Gordon, T.R., 2000. *Gibberella fujikuroi* mating population A and *Fusarium subglutinans* from teosinte species and maize from Mexico and Central America. *Mycological Research*, *104*(7), pp.865-872.

De Vos, L., Van der Nest, M.A., Van der Merwe, N.A., Myburg, A.A., Wingfield, M.J. and Wingfield, B.D., 2011. Genetic analysis of growth, morphology and pathogenicity in the F1 progeny of an interspecific cross between *Fusarium circinatum* and *Fusarium subglutinans*. *Fungal Biology*, 115(9), pp.902-908.

Drenkhan, R., Ganley, B., Martín-García, J., Vahalík, P., Adamson, K., Adamčíková, K., Ahumada, R., Blank, L., Bragança, H., Capretti, P. and Cleary, M., 2020. Global geographic distribution and host range of *Fusarium circinatum*, the causal agent of pine pitch canker. *Forests*, 11(7), p.724.

Dwinell, L.D., Barrows-Broaddus, J.B. and Kuhlman, E.G., 1985. Pitch canker: a disease complex. *Plant Disease*, 69, pp.270-276..

Elvira-Recuenco, M., Pando, V., Berbegal, M., Manzano Muñoz, A., Iturritxa, E. and Raposo, R., 2021. Influence of temperature and moisture duration on pathogenic life history traits of predominant haplotypes of *Fusarium circinatum* on *Pinus* spp. in Spain. *Phytopathology*, 111(11), pp.2002-2009.

Flemming, H.C., Neu, T.R. and Wingender, J. eds., 2016. The perfect slime: microbial extracellular polymeric substances *(EPS)*. IWA publishing.

Flemming, H.C. and Wingender, J., 2010. The biofilm matrix. *Nature reviews microbiology*, 8(9), pp.623-633.

Flemming, H.C., Wingender, J., Griegbe, T. and Mayer, C., 2000. Physico-chemical properties of biofilms. Biofilms: recent advances in their study and control. Amsterdam: *Harwood Academic Publishers*, 2000, pp.19-34.

Foucher, A., Evrard, O., Ficetola, G.F., Gielly, L., Poulain, J., Giguet-Covex, C., Laceby, J.P., Salvador-Blanes, S., Cerdan, O. and Poulenard, J., 2020. Persistence of environmental DNA in cultivated soils: implication of this memory effect for reconstructing the dynamics of land use and cover changes. *Scientific Reports*, 10(1), pp.1-12.

Geffert, A., Geffertova, J. and Dudiak, M., 2019. Direct method of measuring the pH value of wood. *Forests*, 10(10), p.852.

Gordon, T.R., 2006. Pitch canker disease of pines. *Phytopathology*, 96(6), pp.657-659.

Hall-Stoodley, L., Costerton, J.W. and Stoodley, P., 2004. Bacterial biofilms: from the natural environment to infectious diseases. *Nature reviews microbiology*, 2(2), pp.95-108.

Harding, M.W., Marques, L.L., Howard, R.J. and Olson, M.E., 2009. Can filamentous fungi form biofilms?. *Trends in microbiology*, 17(11), pp.475-480.

Harding, M.W., Marques, L.L., Shore, B. and Daniels, G.C., 2017. The significance of fungal biofilms in association with plants and soils. *Biofilms in Plant and Soil Health*, pp.131-149.

Hausner, M. and Wuertz, S., 1999. High rates of conjugation in bacterial biofilms as determined by quantitative in situ analysis. *Applied and environmental microbiology*, 65(8), pp.3710-3713.

Herkert, P.F., Al-Hatmi, A.M., de Oliveira Salvador, G.L., Muro, M.D., Pinheiro, R.L., Nucci, M., Queiroz-Telles, F., de Hoog, G.S. and Meis, J.F., 2019. Molecular characterization and antifungal susceptibility of clinical Fusarium species from Brazil. *Frontiers in microbiology*, 10, p.737.

Hernandez-Escribano, L., Iturritxa, E., Aragonés, A., Mesanza, N., Berbegal, M., Raposo, R. and Elvira-Recuenco, M., 2018. Root infection of canker pathogens, *Fusarium circinatum* and *Diplodia sapinea*, in asymptomatic trees in *Pinus radiata* and *Pinus pinaster* plantations. *Forests*, 9(3), p.128.

Nett, J.E., Crawford, K., Marchillo, K. and Andes, D.R., 2010. Role of Fks1p and matrix glucan in *Candida albicans* biofilm resistance to an echinocandin, pyrimidine, and polyene. *Antimicrobial agents and chemotherapy*, *54*(8), pp.3505-3508.

Ommen, P., Zobek, N. and Meyer, R.L., 2017. Quantification of biofilm biomass by staining: Non-toxic safranin can replace the popular crystal violet. *Journal of microbiological methods*, *141*, pp.87-89.

Martínez-Álvarez, P., Pando, V. and Diez, J.J., 2014. Alternative species to replace Monterey pine plantations affected by pitch canker caused by *Fusarium circinatum* in northern S pain. *Plant pathology*, 63(5), pp.1086-1094..

Martín-García, J., Lukačevičová, A., Flores-Pacheco, J.A., Diez, J.J. and Dvořák, M., 2018. Evaluation of the susceptibility of several Czech conifer provenances to *Fusarium circinatum*. *Forests*, 9(2), p.72.

Martins, M., Uppuluri, P., Thomas, D.P., Cleary, I.A., Henriques, M., Lopez-Ribot, J.L. and Oliveira, R., 2010. Presence of extracellular DNA in the *Candida albicans* biofilm matrix and its contribution to biofilms. *Mycopathologia*, 169, pp.323-331.

McDougald, D., Rice, S.A., Barraud, N., Steinberg, P.D. and Kjelleberg, S., 2012. Should we stay or should we go: mechanisms and ecological consequences for biofilm dispersal. *Nature Reviews Microbiology*, *10*(1), pp.39-50.

Mitchell, K.F., Zarnowski, R. and Andes, D.R., 2016. Fungal super glue: the biofilm matrix and its composition, assembly, and functions. *PLoS pathogens*, 12(9), p.e1005828.

Motaung, T.E., Peremore, C., Wingfield, B. and Steenkamp, E., 2020. Plant-associated fungal biofilms—knowns and unknowns. *FEMS Microbiology Ecology*, 96(12), p.fiaa224.

Monticolo, F., Palomba, E., Termolino, P., Chiaiese, P., De Alteriis, E., Mazzoleni, S. and Chiusano, M.L., 2020. The role of DNA in the extracellular environment: a focus on NETs, RETs and biofilms. *Frontiers in Plant Science*, *11*, p.589837.

Mowat, E., Butcher, J., Lang, S., Williams, C. and Ramage, G., 2007. Development of a simple model for studying the effects of antifungal agents on multicellular communities of *Aspergillus fumigatus*. *Journal of Medical Microbiology*, *56*(9), pp.1205-1212.

Mowat E, Williams C, Jones B, McChlery S & Ramage G (2009). The characteristics of *Aspergillus fumigatus* mycetoma development: is this a biofilm? *Medical Mycology*, 47: S120–S126.

Mukherjee, P.K., Chandra, J., Yu, C., Sun, Y., Pearlman, E. and Ghannoum, M.A., 2012. Characterization of *Fusarium keratitis* outbreak isolates: contribution of biofilms to antimicrobial resistance and pathogenesis. *Investigative Ophthalmology & Visual Science*, 53(8), pp.4450-4457.

Mulcahy, H., Charron-Mazenod, L. and Lewenza, S., 2008. Extracellular DNA chelates cations and induces antibiotic resistance in *Pseudomonas aeruginosa* biofilms. *PLoS Pathogens*, 4(11), p.e1000213.

Nirenberg HI, O'Donnell K, 1998. New Fusarium species and combinations within the *Gibberella fujikuroi* species complex. *Mycologia*, 90, pp434-458.

Luo, J., Chu, X., Jie, J., Sun, Y., Guan, Q., Li, D., Luo, Z.Q. and Song, L., 2023. *Acinetobacter baumannii* Kills Fungi via a Type VI DNase Effector. *Mbio*, pp.e03420-22.

Odds, F.C., Brown, A.J. and Gow, N.A., 2003. Antifungal agents: mechanisms of action. *Trends in Microbiology*, 11(6), pp.272-279.

Oliveira, H.M., Santos, C., Paterson, R.R.M., Gusmão, N.B. and Lima, N., 2016. Fungi from a groundwater-fed drinking water supply system in Brazil. *International Journal of Environmental Research and Public Health*, 13(3), p.304.

Oliveira, R.V.D.D., Albuquerque, Y.E., Spolidorio, D.M.P., Koga-Ito, C.Y., Giro, E.M.A. and Brighenti, F.L., 2016. Effect of dietary sugars on dual-species biofilms of *Streptococcus mutans* and *Streptococcus sobrinus*–a pilot study. *Revista de Odontologia da UNESP*, 45, pp.90-96.

Peeters, E., Nelis, H.J. and Coenye, T., 2008. Comparison of multiple methods for quantification of microbial biofilms grown in microtiter plates. *Journal of microbiological methods*, *72*(2), pp.157-165.

Peiqian, L., Xiaoming, P., Huifang, S., Jingxin, Z., Ning, H. and Birun, L., 2014. Biofilm formation by *Fusarium oxysporum f. sp. cucumerinum* and susceptibility to environmental stress. *FEMS Microbiology Letters*, *350*(2), pp.138-145.

Peng, D., 2016. Biofilm formation of Salmonella. *Microbial biofilms-importance and applications*, *556*.

Peremore, C., Wingfield, B., Santana, Q., Steenkamp, E.T. and Motaung, T.E., 2022. Biofilm characterization in the maize pathogen, *Fusarium verticillioides*. *bioRxiv*, pp.2022-11.

Perumal, P., Mekala, S. and Chaffin, W.L., 2007. Role for cell density in antifungal drug resistance in *Candida albicans* biofilms. *Antimicrobial Agents and Chemotherapy*, 51(7), pp.2454-2463.

Phasha, M.M., Wingfield, B.D., Wingfield, M.J., Coetzee, M.P.A., Hammerbacher, A. and Steenkamp, E.T., 2021. Deciphering the effect of FUB1 disruption on fusaric acid production and pathogenicity in *Fusarium circinatum*. *Fungal Biology*, *125*(12), pp.1036-1047.

Phasha, M.M., Wingfield, M.J., Wingfield, B.D., Coetzee, M.P.A., Hallen-Adams, H., Fru, F., Swalarsk-Parry, B.S., Yilmaz, N., Duong, T.A. and Steenkamp, E.T., 2021. Ras2 is important for growth and pathogenicity in *Fusarium circinatum*. *Fungal Genetics and Biology*, *150*, p.103541.

Rajendran, R., Sherry, L., Lappin, D.F., Nile, C.J., Smith, K., Williams, C., Munro, C.A. and Ramage, G., 2014. Extracellular DNA release confers heterogeneity in *Candida albicans* biofilm formation. *BMC Microbiology*, 14(1), pp.1-9.

Rajendran, R., Williams, C., Lappin, D.F., Millington, O., Martins, M. and Ramage, G., 2013. Extracellular DNA release acts as an antifungal resistance mechanism in mature *Aspergillus fumigatus* biofilms. *Eukaryotic cell*, 12(3), pp.420-429.

Ramage, G., Mowat, E., Jones, B., Williams, C. and Lopez-Ribot, J., 2009. Our current understanding of fungal biofilms. *Critical Reviews in Microbiology*, 35(4), pp.340-355.

Ramey, B.E., Koutsoudis, M., von Bodman, S.B. and Fuqua, C., 2004. Biofilm formation in plant–microbe associations. *Current Opinion in Microbiology*, 7(6), pp.602-609.

Robbins, N., Caplan, T. and Cowen, L.E., 2017. Molecular evolution of antifungal drug resistance. *Annual Review of Microbiology*, 71, pp.753-775.

Roehm, N.W., Rodgers, G.H., Hatfield, S.M. and Glasebrook, A.L., 1991. An improved colorimetric assay for cell proliferation and viability utilizing the tetrazolium salt XTT. *Journal of immunological methods*, 142(2), pp.257-265.

Romero, D., Aguilar, C., Losick, R. and Kolter, R., 2010. Amyloid fibers provide structural integrity to *Bacillus subtilis* biofilms. *Proceedings of the National Academy of Sciences*, 107(5), pp.2230-2234.

Sardi, J.D.C.O., Pitangui, N.D.S., Rodríguez-Arellanes, G., Taylor, M.L., Fusco-Almeida, A.M. and Mendes-Giannini, M.J.S., 2014. Highlights in pathogenic fungal biofilms. *Revista iberoamericana de micologia*, 31(1), pp.22-29.

Sati, S.C. and Bisht, S., 2006. Utilization of various carbon sources for the growth of waterborne conidial fungi. *Mycologia*, 98(5), pp.678-681.

Sav, H., Rafati, H., Öz, Y., Dalyan-Cilo, B., Ener, B., Mohammadi, F., Ilkit, M., Van Diepeningen, A.D. and Seyedmousavi, S., 2018. Biofilm formation and resistance to fungicides in clinically relevant members of the fungal genus Fusarium. *Journal of Fungi*, 4(1), p.16.

Schlafer, S., Garcia, J., Meyer, R.L., Vaeth, M. and Neuhaus, K.W., 2018. Effect of DNase treatment on adhesion and early biofilm formation of *Enterococcus faecalis*. *European Endodontic Journal*, 3(2), p.82.

Seidler, M.J., Salvenmoser, S. and Müller, F.M.C., 2008. *Aspergillus fumigatus* forms biofilms with reduced antifungal drug susceptibility on bronchial epithelial cells. *Antimicrobial Agents and Chemotherapy*, 52(11), pp.4130-4136.

Sheppard, D.C. and Howell, P.L., 2016. Biofilm exopolysaccharides of pathogenic fungi: lessons from bacteria. *Journal of Biological Chemistry*, 291(24), pp.12529-12537.

Silva, S., Henriques, M., Martins, A., Oliveira, R., Williams, D. and Azeredo, J., 2009. Biofilms of non-*Candida albicans* Candida species: quantification, structure and matrix composition. *Sabouraudia,* 47(7), pp.681-689.

Singh, R., Shivaprakash, M.R. and Chakrabarti, A., 2011. Biofilm formation by zygomycetes: quantification, structure and matrix composition. *Microbiology*, 157(9), pp.2611-2618.

Souli, M. and Giamarellou, H., 1998. Effects of slime produced by clinical isolates of coagulase-negative staphylococci on activities of various antimicrobial agents. *Antimicrobial Agents and Chemotherapy*, *42*(4), pp.939-941.

Stoodley, P., Sauer, K., Davies, D.G. and Costerton, J.W., 2002. Biofilms as complex differentiated communities. *Annual Review of Microbiology*, 56(1), pp.187-209.

Storer, A.J., Gordon, T.R. and Clark, S.L., 1998. Association of the pitch canker fungus, *Fusarium subglutinans f.* sp*. pini,* with Monterey pine seeds and seedlings in California. *Plant Pathology*, 47(5), pp.649-656.

Sutherland, I.W., 2001. Biofilm exopolysaccharides: a strong and sticky framework. *Microbiology*, 147(1), pp.3-9.

Swalarsk-Parry, B.S., Steenkamp, E.T., van Wyk, S., Santana, Q.C., van der Nest, M.A., Hammerbacher, A., Wingfield, B.D. and De Vos, L., 2022. Identification and Characterization of a QTL for Growth of *Fusarium circinatum* on Pine-Based Medium. *Journal of Fungi*, *8*(11), p.1214.

Swett, C.L. and Gordon, T.R., 2012. First report of grass species (Poaceae) as naturally occurring hosts of the pine pathogen *Gibberella circinata*. *Plant Disease*, 96(6), pp.908-908.

Swett, C.L., Porter, B., Fourie, G., Steenkamp, E.T., Gordon, T.R. and Wingfield, M.J., 2014. Association of the pitch canker pathogen *Fusarium circinatum* with grass hosts in commercial pine production areas of South Africa. Southern Forests: *A Journal of Forest Science*, 76(3), pp.161-166.

Tetz, G.V., Artemenko, N.K. and Tetz, V.V., 2009. Effect of DNase and antibiotics on biofilm characteristics. *Antimicrobial agents and chemotherapy*, 53(3), pp.1204-1209.

Tini, F., Beccari, G., Onofri, A., Ciavatta, E., Gardiner, D.M. and Covarelli, L., 2020. Fungicides may have differential efficacies towards the main causal agents of Fusarium head blight of wheat. *Pest Management Science*, 76(11), pp.3738-3748.

Van Duijkeren, E., Schink, A.K., Roberts, M.C., Wang, Y. and Schwarz, S., 2018. Mechanisms of bacterial resistance to antimicrobial agents. *Microbiology Spectrum*, 6(2), pp.6-2.

Wingfield MJ, Hammerbacher A, Ganley RJ, Steenkamp ET, Gordon TR, Wingfield BD, Coutinho TA, 2008. Pitch canker caused by *Fusarium circinatum*: a growing threat to pine plantations and forests worldwide. *Australasian Plant Pathology*, 37, 319-334.

Xu, Z., Liang, Y., Lin, S., Chen, D., Li, B., Li, L. and Deng, Y., 2016. Crystal violet and XTT assays on *Staphylococcus aureus* biofilm quantification. *Current Microbiology*, 73(4), pp.474-482.

Yang, K., Wang, L., Cao, X., Gu, Z., Zhao, G., Ran, M., Yan, Y., Yan, J., Xu, L., Gao, C. and Yang, M., 2022. The Origin, Function, Distribution, Quantification, and Research Advances of Extracellular DNA. *International Journal of Molecular Sciences*, 23(22), p.13690.

Figures

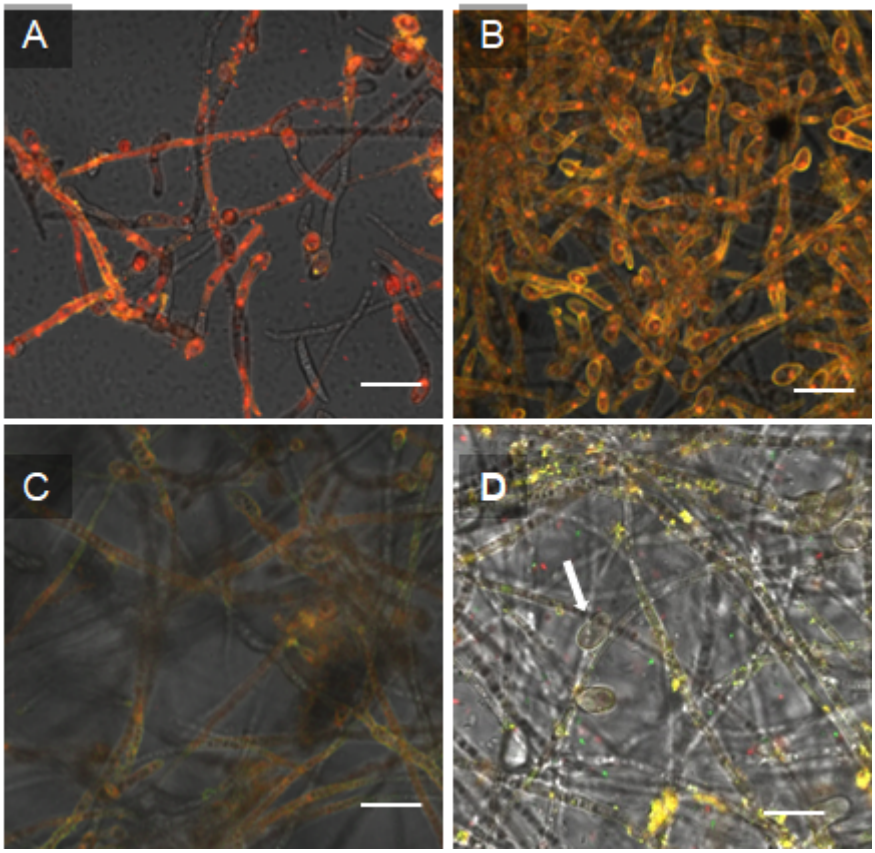

Figure 1

Confocal laser scanning microscopic imaging of *Fusarium circinatum* biofilms following growth in ¼ Potato Dextrose Broth (PDB). the fluorescence cell wall polysaccharide-binding A-Alexa Fluor 488 conjugate (green) and the metabolically active cell binding Fun 1(red). *Fusarium circinatum* biofilms were dually stained over time. The different phases of biofilm formation of the FSP34 isolate were observed including (A-B) adhesion and microconidia phase, spores exhibiting metabolic activities (red-orange), (C-D) maturation and dispersal phase exhibiting extracellular polymeric matrix (ECM, yellow-green) production and dispersal of conidia (white arrow). Scale bar 10 µm is representative of this micrographs.

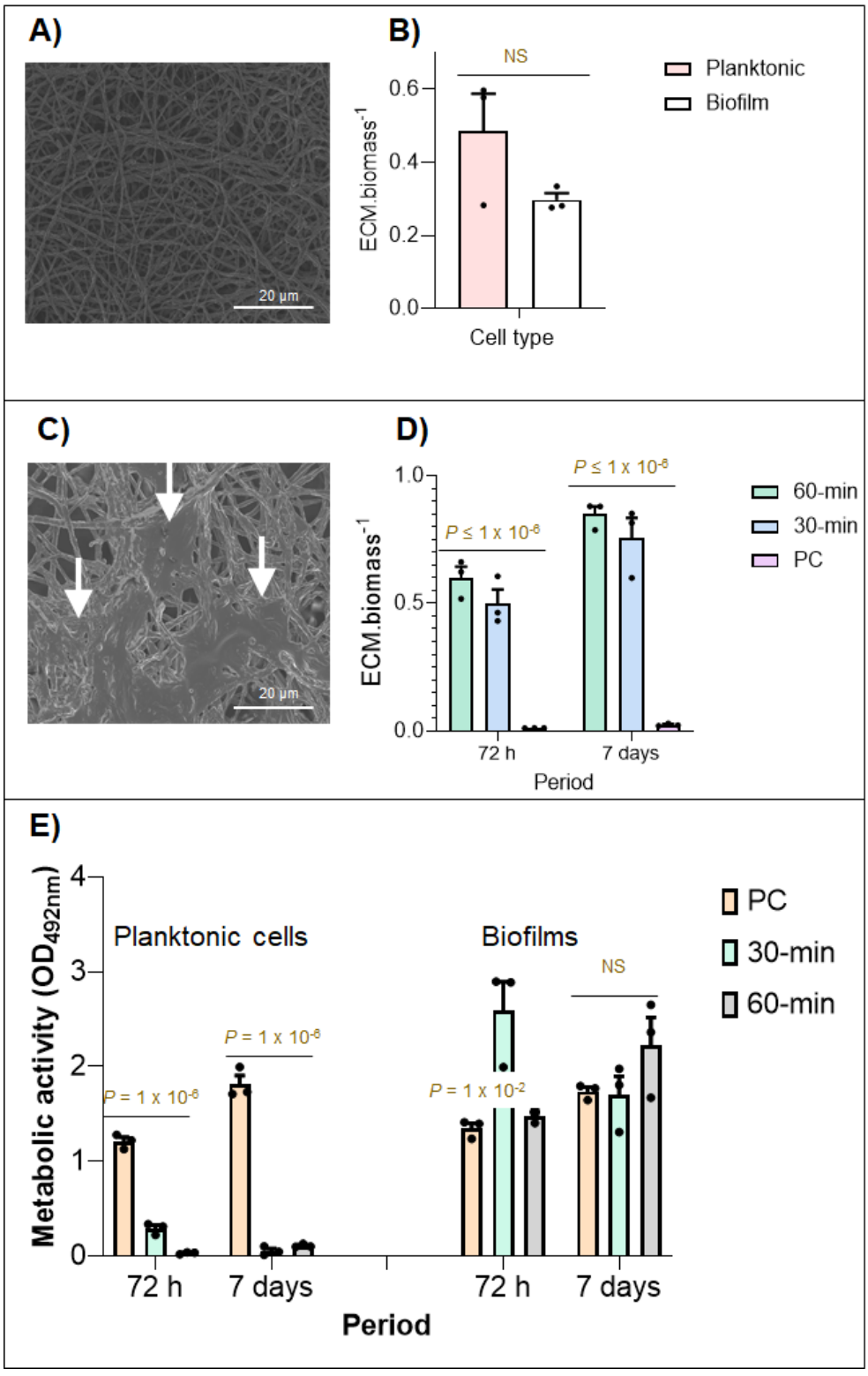

Figure 2

A: Effects of heat-shock (45 oC for 30 ad 60 minutes) on *Fusarium circinatum* planktonic cells and preformed biofilms. Growth in the absence **(A-B)** and presence **(C-D)** of heat. **A:** A complex aggregated growth of hyphal bundles**. B:** Planktonic cells and biofilm formation quantified in terms of extracellular matrix (ECM) produced per unit of biofilm biomass (ECMOD530, biomassOD540) at day 7 following incubation. **C:**Hyphae embedded in a secreted ECM (white arrows). **D:** ECM quantification following heat-

shock. **E:** Effects on themetabolic activity ofplanktonic cells and preformed biofilms. NS-not significant, PC-positive control.

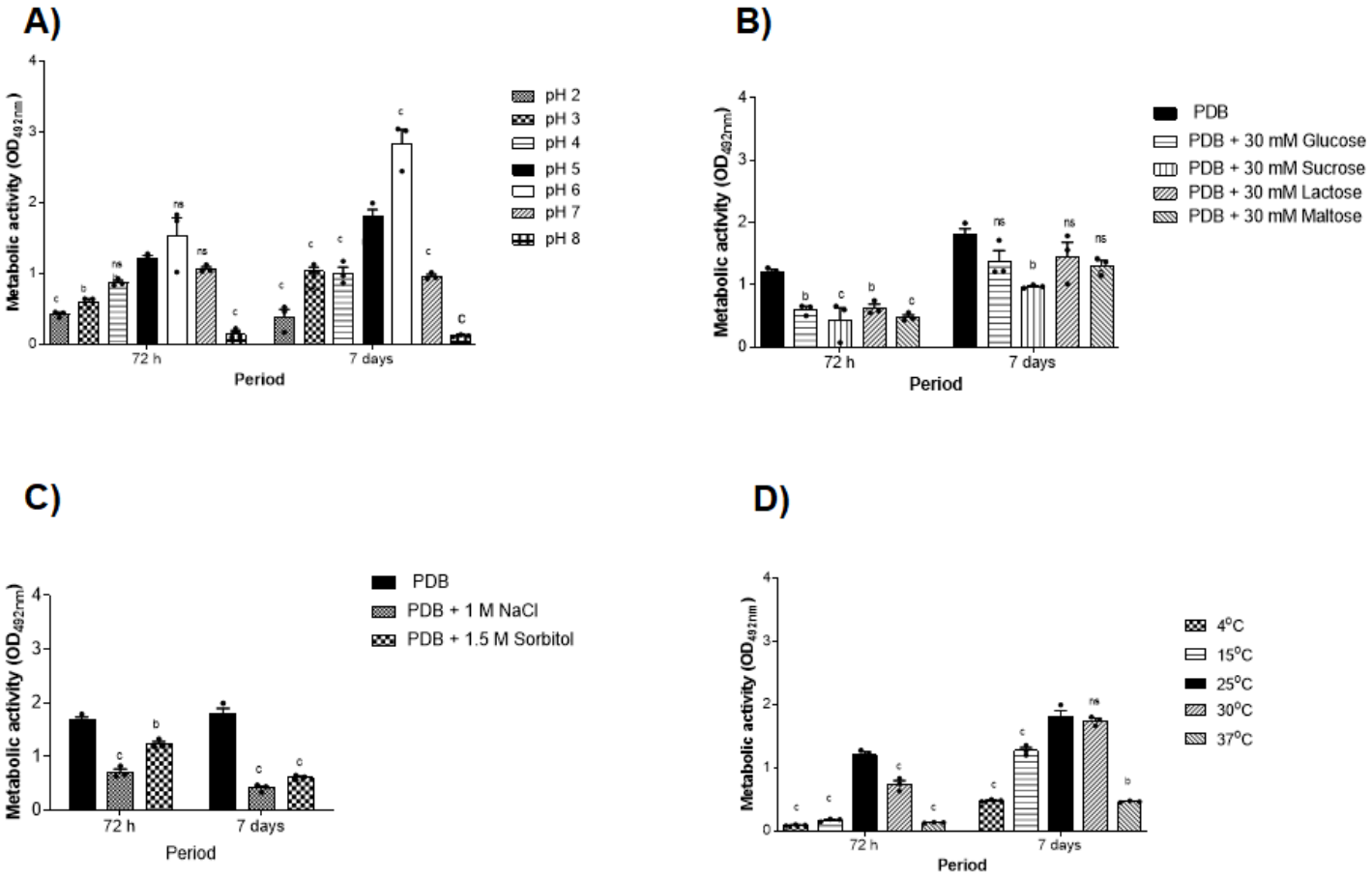

Figure 3

Impact of environmental cues in *Fusarium circinatum*biofilm formation assessed in PDB (potato dextrose broth). The formation of biofilms was observed under different conditions using XTT assay including **A**-pH, B-sugars **C**-osmotic stress (NaCl) and **D**-temperature. Statistical significance levels were defined as P > 0.05 = not significant (ns) and $p < 0.01$ (a, b, c).

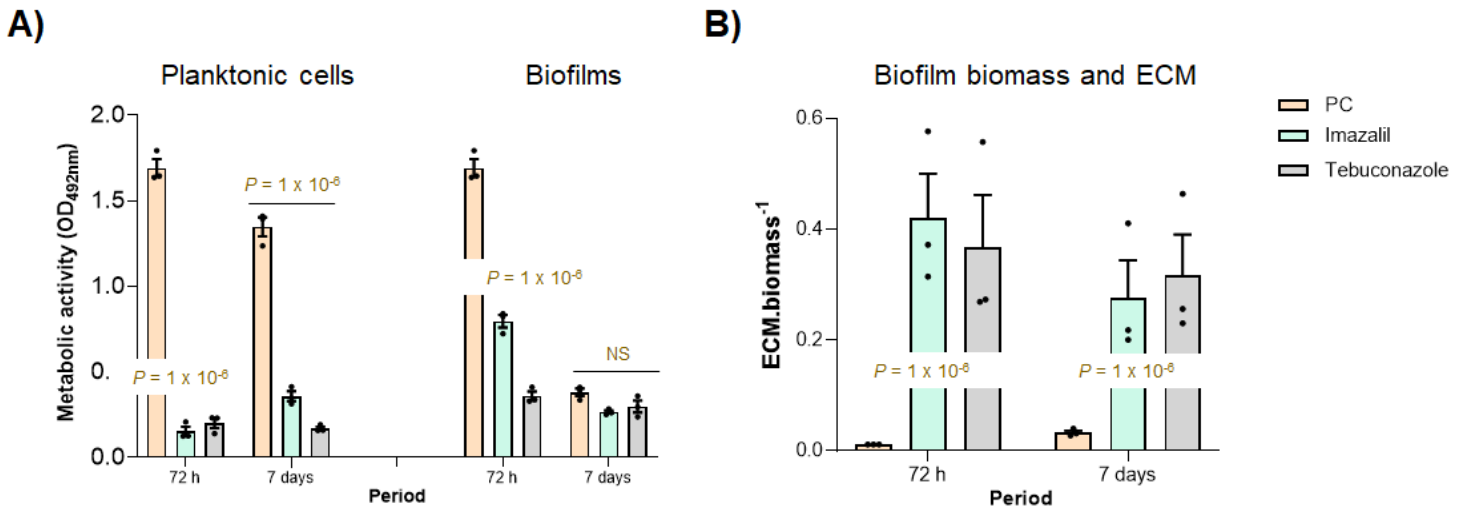

Figure 4

A: The impact of Imazalil and Tebuconazole, both at an inhibitory concentration that reduces viability by 50% (Ic50), on the metabolic activity of planktonic cells and biofilms. **B:** Quantification of the extracellular matrix (ECM) per unit of biomass secreted by biofilms following exposure to a fungicidal treatment. NS- not significant, PC-positive control.

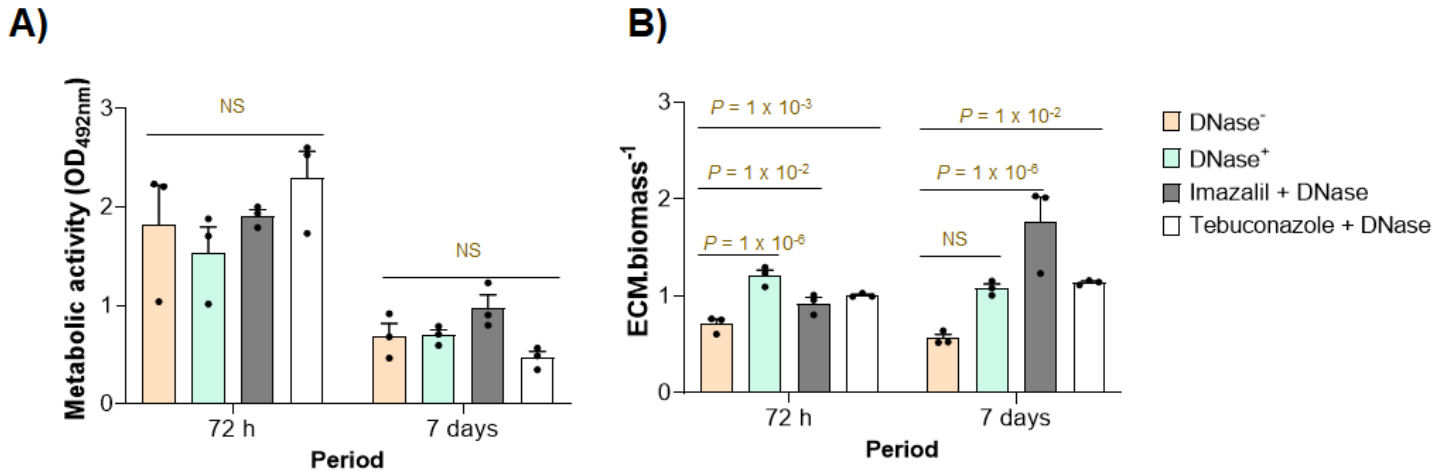

Figure 5

The effects of DNase I treatment on pre-formed biofilms. **A:** Effect on metabolic activity. **B:** Effect on extracellular matric production per unit of biofilm biomass. DNase- - negative control.

Supplementary Files

This is a list of supplementary files associated with this preprint. Click to download.

- FigS1.png

- FigS2.png
- FigS3.png
- TableS1.png